Available online at www.sciencedirect.com

ScienceDirect

journal homepage: http://www.elsevier.com/locate/acme

Original Research Article

Large deflections of nonlinearly elastic functionally graded composite beams

M. Sitar [a,*], F. Kosel [a], M. Brojan [b]

[a] Laboratory for Nonlinear Mechanics, Faculty of Mechanical Engineering, University of Ljubljana, Askerceva 6, SI-1000, Ljubljana, Slovenia

[b] Department of Mechanical Engineering, Massachusetts Institute of Technology, 77 Massachusetts Avenue, Cambridge, MA 02139-4307, United States

ARTICLE INFO

Article history:
Received 28 January 2013
Accepted 20 November 2013
Available online 15 December 2013

Keywords:
Lamina
Functionally graded material
Material nonlinearity
Geometrical nonlinearity
Numerical analysis

ABSTRACT

The paper discusses governing differential equation for determining large deflections of slender, non-homogeneous beam subjected to a combined loading and composed of a finite number of laminae, which are made of nonlinearly elastic, modified Ludwick's type of material with different stress–strain relations in tension and compression domain. The material properties are varying arbitrarily through the beam's thickness. When the thickness of laminae is sufficiently small and the variation of mechanical properties is close to continuous, the beam can be considered as made of functionally graded material (FGM). The derived equations are solved numerically and tested on several examples. From a comparison of the results obtained and those found in the literature a good agreement was observed.

© 2013 Politechnika Wrocławska. Published by Elsevier Urban & Partner Sp. z o.o. All rights reserved.

1. Introduction

The ability to compute deflections either for estimation of rigidity of an element and/or structure, comparison of theoretical and experimental results, computation of allowable deflections, or a post-buckling analysis, has always been desired. Large deflections of flexible elements have been in the center of attention to a number of researchers who tried to understand, model and determine their states. There exist many assumptions which gave rise to theories for modeling large deflections. Namely, for slender beams, where the influence of shear stresses and the inner axial force can be neglected in comparison to the dominating inner bending moment, Euler–Bernoulli beam theory is the most appropriate and frequently used. For thicker beams more accurate kinematic descriptions of the beams that consider the presence of shear stresses can be used, e.g. Timoshenko's or Reissner's description.

In recent years, effects of geometrical nonlinearities are being complemented by studies of material nonlinearities. In particular, Lewis and Monasa [1] and Lee [2] dealt with large deflections of thin cantilever beams of non-linear Ludwick type materials subjected to an end moment and combined loading consisting of uniformly distributed load and one vertical point load at the free end, respectively. Large deflections of a nonlinearly non-prismatic cantilever beam subjected to an end moment and static stability of nonlinearly elastic Euler's columns made from materials obeying the modified Ludwick constitutive law was investigated by Brojan et al. [3,4], respectively. Furthermore, in the works by Baykara

* *Corresponding author*. Tel.: +386 1 4771 517; fax: +386 1 2518 567.
E-mail address: matej.sitar@fs.uni-lj.si (M. Sitar).

1644-9665/$ – see front matter © 2013 Politechnika Wrocławska. Published by Elsevier Urban & Partner Sp. z o.o. All rights reserved.
http://dx.doi.org/10.1016/j.acme.2013.11.007

et al. [5] and Brojan et al. [6], nonlinear bimodulus material was considered. Al-Sadder and Shatarat [7] developed a technique for a large deflection problem of a prismatic composite cantilever beam made of two different nonlinear elastic materials and subjected to an inclined tip concentrated force.

In the last two decades, demands for advanced materials that are capable of withstanding high temperature environment and exhibiting adequate mechanical performance, have stimulated the study, development and fabrication technologies of functionally graded materials (FGMs). With FGMs, where the material properties (e.g. Young's modulus, density, heat conductivity) of two or more constituents continuously vary as a function with respect to prescribed spatial directions, the desired performance of components can be tuned. Today FGMs have become widely used in aerospace, aircraft, automotive and civil structural, thermal, optical and electronic applications.

One of the first studies of modeling and design of multilayered and graded materials was published by Suresh [8]. Sankar [9] obtained an elasticity solution for a simply supported FGM beam. Furthermore, Zhong and Yu [10,11] presented analytical solutions for orthotropic functionally graded beams with arbitrary elastic moduli variations along the thickness direction under different boundary conditions. Using the displacement function method an analytical solution of a FGM beam with arbitrary graded material properties was investigated by Nie et al. [12]. A new beam element based on the first order shear deformation theory to study the thermoelastic behaviour of FGM beam structures was developed by Chakraborty et al. [13]. Li [14] gave a unified approach for analyzing static and dynamic behaviours of FGM Timoshenko and Euler–Bernoulli beams. Kang and Li [15,16] investigated the effects of depth-depended Young's modulus and the non-linearity parameters on the large deflections of the FGM beam. Similar problem was investigated by Kocatürk et al. [18], where Timoshenko beam theory and FEM are used. Soleimani and Saddatfar [19,20] presented large deflections of axially functionally graded beam using shooting method.

The present paper considers the problem of large deflections of slender, non-homogeneous cantilever beam subjected to a combined loading consisting of the distributed continuous loads and point loads at the free end. The material of which the beam is made is assumed to be nonlinearly elastic and only locally homogeneous. The mechanical properties are varying arbitrarily through the beam's thickness with different stress–strain relations in tensile and compressive domain.

The main focus of the paper is to derive the governing differential equations for determining large deflections of the beam composed of a finite number of laminae. Each lamina is in general characterized by their constant thickness and material properties. Some of the results obtained in this study are compared to those found in the available literature.

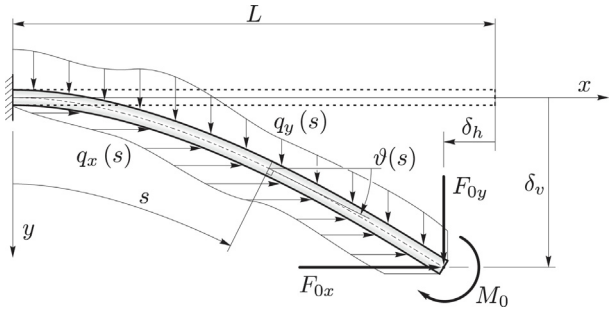

Fig. 1 – Deflected state of the cantilever FGM beam.

2. Definition of the problem

Consider a slender, initially straight elastic cantilever FGM beam of length L and uniform rectangular cross-section of thickness h and width b. The beam is subjected to the distributed continuous loads $q_x(s)$, $q_y(s)$ and point loads at the free end, i.e. F_{0x}, F_{0y} and M_0, see Fig. 1. This FGM beam is composed of n laminae which are different in general, each characterized by their constant thickness and material properties.

The mathematical model of the discussed problem is based on the elastica theory with the following assumptions:

- the material of which each lamina is made is assumed to be incompressible, isotropic, nonlinearly elastic and homogeneous. No slip condition between particular laminae is considered. They are rigidly bonded together;
- different nonlinear relations between the stress and strain in tensile and compressive domain are considered, see Fig. 3;
- the stress–strain relationship is assumed to be governed by the modified Ludwick constitutive model, mathematically described by the following expression

$$\sigma_i(\varepsilon) = \begin{cases} \sigma_{t,i}(\varepsilon) = E_{t,i}\left((\varepsilon + \varepsilon_{0t,i})^{1/k_{t,i}} - \varepsilon_{0t,i}^{1/k_{t,i}}\right) & \text{for } \varepsilon \geq 0, \\ \sigma_{c,i}(\varepsilon) = -E_{c,i}\left((-\varepsilon + \varepsilon_{0c,i})^{1/k_{c,i}} - \varepsilon_{0c,i}^{1/k_{c,i}}\right) & \text{for } \varepsilon < 0. \end{cases} \quad (1)$$

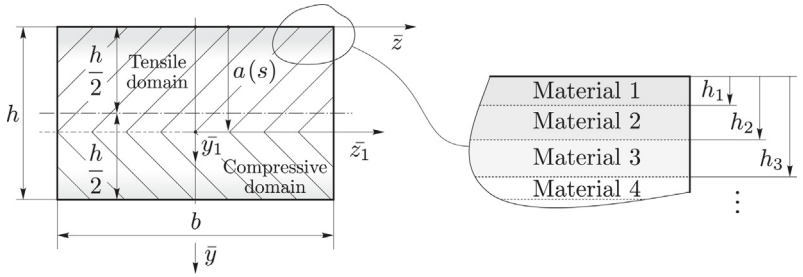

Fig. 2 – Cross-section of the FGM cantilever beam.

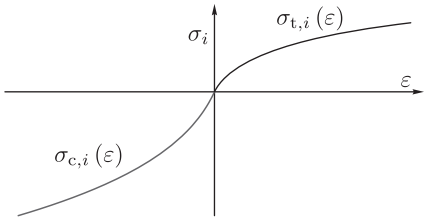

Fig. 3 – Stress–strain diagram of ith lamina.

for $i \in \{1, 2, \ldots, n\}$, where $\sigma_{t,i}(\varepsilon)$ and $\sigma_{c,i}(\varepsilon)$ represent stress–strain relations and $E_{t,i}$, $\varepsilon_{0t,i}$, $k_{t,i}$ and $E_{c,i}$, $\varepsilon_{0c,i}$, $k_{c,i}$ represent material constants in tensile and compressive domain of the ith lamina, respectively, cf. Refs. [17,3]. In practice, the material constants are obtained from experimental data;

- shear stresses in the beam are negligible compared to normal stresses since the length–height ratio of the beam is large;
- Euler–Bernoulli hypothesis, which states that cross-sections which are perpendicular to the neutral axis before deformation, remain plain and perpendicular to the neutral axis in the deformed state of the beam and do not change their shape and area.

The Cartesian coordinate system $xy0$ is introduced such that the x-axis coincides with the longitudinal axis of the undeformed beam and the coordinate origin is located at its clamped end. Let s, $0 \le s \le L$, be the curvilinear coordinate along the neutral axis measured from the clamped end of the beam and $\vartheta(s)$ the angle of inclination at local point s, see Fig. 1 and Fig. 5. Here δ_v and δ_h designate vertical and horizontal deflection of the free end with respect to the unloaded configuration.

3. Problem formulation

3.1. *Inner axial force*

The inner axial force is determined by the known expression, i.e.

$$N(s) = \int_A \sigma(\varepsilon)\, dA = \int_{A_t(s)} \sigma_t(\varepsilon)\, dA + \int_{A_c(s)} \sigma_c(\varepsilon)\, dA. \tag{2}$$

Since in general the position of the neutral axis is unknown, there exists n possible variants of the expression for the inner axial force, see Fig. 4. In the present paper only the positive curvature of the deformed neutral axis is taken into consideration. Due to the description above, index j is the function of the neutral axis position $a(s)$,

$$j = \begin{cases} 1 & \text{if } h_{t,1} \le a(s) < h_{b,1}, \\ \vdots & \\ i-1 & \text{if } h_{t,i-1} \le a(s) < h_{b,i-1}, \\ i & \text{if } h_{t,i} \le a(s) < h_{b,i}, \\ i+1 & \text{if } h_{t,i+1} \le a(s) < h_{b,i+1}, \\ \vdots & \\ n & \text{if } h_{t,n} \le a(s) \le h_{b,n}. \end{cases} \tag{3}$$

where $h_{t,i}$ and $h_{b,i}$ are (distances to) the top and bottom surface of the ith lamina measured from the top surface of the beam ($\bar{y} = 0$), respectively, cf. Fig. 4,

$$h_{t,1} = 0, \quad h_{t,i} = h_{i-1}, \quad h_{b,i} = h_i. \tag{4}$$

For the jth variant it follows

$$N_j(s) = \sum_{i=1}^{j-1} \int_{h_{t,i}}^{h_{b,i}} \sigma_{t,i}(\varepsilon) b\, d\bar{y} + \int_{h_{t,j}}^{a(s)} \sigma_{t,j}(\varepsilon) b\, d\bar{y} + \int_{a(s)}^{h_{b,j}} \sigma_{c,j}(\varepsilon) b\, d\bar{y} + \sum_{i=j+1}^{n} \int_{h_{t,i}}^{h_{b,i}} \sigma_{c,i}(\varepsilon) b\, d\bar{y}. \tag{5}$$

The known normal strain–curvature expression is given by $\varepsilon = -\rho(s)^{-1}\overline{y_1}$, where $\rho(s)$ is the radius of curvature of the neutral axis and the coordinate $\overline{y_1}$ is measured from the neutral axis position, Fig. 2. Due to the coordinate $\bar{y}$, which is measured from the top surface of the beam, the normal strain–curvature expression can be written as

$$\varepsilon(\bar{y}) = \frac{a(s) - \bar{y}}{\rho(s)}. \tag{6}$$

Substituting the normal strain–curvature expression (6) and geometrical relation $\rho^{-1}(s) = \vartheta'(s)$ into Eq. (5) leads to

$$N_j(s) = A_j + \frac{b}{\vartheta'(s)} B_{1,j}, \tag{7}$$

where

$$A_j = A_{t,j} + A_{c,j} + A_{tc,j}, \tag{8}$$

$$A_{t,j} = -\sum_{i=1}^{j-1} b E_{t,i} \varepsilon_{0t,i}^{1/k_{t,i}} (h_{b,i} - h_{t,i}), \tag{9}$$

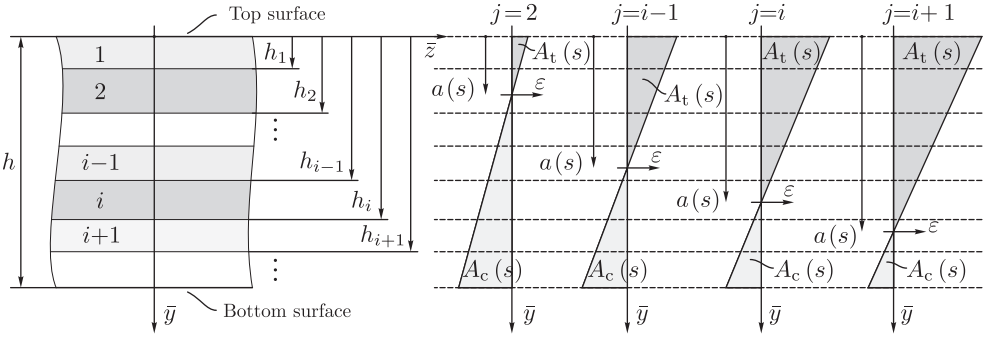

Fig. 4 – Some possible variants of the strain distributed over the beam's cross-section due to the neutral axis position.

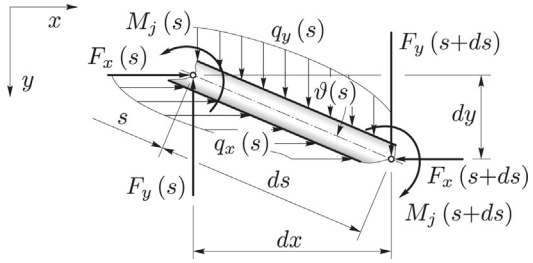

Fig. 5 – Infinitesimal element of the deflected beam.

$$A_{c,j} = \sum_{i=j+1}^{n} bE_{c,i}\varepsilon_{0c,i}^{1/k_{c,i}}(h_{b,i} - h_{t,i}), \tag{10}$$

$$A_{tc,j} = -bE_{t,j}\varepsilon_{0t,j}^{1/k_{t,j}}(a(s) - h_{t,j}) + bE_{c,j}\varepsilon_{0c,j}^{1/k_{c,j}}(h_{b,j} - a(s)), \tag{11}$$

$$B_{1,j} = B_{1t,j} + B_{1c,j} + B_{1tc,j}, \tag{12}$$

$$B_{1t,j} = -\sum_{i=1}^{j-1} \frac{E_{t,i}k_{t,i}}{1+k_{t,i}}\left(C_{tb,i}^{1+1/k_{t,i}} - C_{tt,i}^{1+1/k_{t,i}}\right), \tag{13}$$

$$B_{1c,j} = -\sum_{i=j+1}^{n} \frac{E_{c,i}k_{c,i}}{1+k_{c,i}}\left(C_{cb,i}^{1+1/k_{c,i}} - C_{ct,i}^{1+1/k_{c,i}}\right), \tag{14}$$

$$B_{1tc,j} = -\frac{E_{t,j}k_{t,j}}{1+k_{t,j}}\left(\varepsilon_{0t,j}^{1+1/k_{t,j}} - C_{tt,j}^{1+1/k_{t,j}}\right) - \frac{E_{c,j}k_{c,j}}{1+k_{c,j}} \times \left(C_{cb,j}^{1+1/k_{c,j}} - \varepsilon_{0c,j}^{1+1/k_{c,j}}\right), \tag{15}$$

$$C_{tt,i} = \varepsilon_{0t,i} + (-h_{t,i} + a(s))\vartheta'(s), \tag{16}$$

$$C_{tb,i} = \varepsilon_{0t,i} + (-h_{b,i} + a(s))\vartheta'(s), \tag{17}$$

$$C_{ct,i} = \varepsilon_{0c,i} + (h_{t,i} - a(s))\vartheta'(s), \tag{18}$$

$$C_{cb,i} = \varepsilon_{0c,i} + (h_{b,i} - a(s))\vartheta'(s) \tag{19}$$

and "′" denotes differentiation with respect to variable s.

3.2. *Inner bending moment*

The inner bending moment is determined by the following expression,

$$M(s) = -\int_A \sigma(\varepsilon)\bar{y}\,dA = -\int_{A_t(s)} \sigma_t(\varepsilon)\bar{y}\,dA - \int_{A_c(s)} \sigma_c(\varepsilon)\bar{y}\,dA. \tag{20}$$

According to the unknown position of the neutral axis, as before, n possible variants of the expression for the inner bending moment can be assumed, Fig. 4. For the jth variant it follows

$$M_j(s) = -\sum_{i=1}^{j-1}\int_{h_{t,i}}^{h_{b,i}} \sigma_{t,i}(\varepsilon)\bar{y}b\,d\bar{y} - \int_{h_{t,j}}^{a(s)} \sigma_{t,j}(\varepsilon)\bar{y}b\,d\bar{y} - \int_{a(s)}^{h_{b,j}} \sigma_{c,j}(\varepsilon)\bar{y}b\,d\bar{y} - \sum_{i=j+1}^{n}\int_{h_{t,i}}^{h_{b,i}} \sigma_{c,i}(\varepsilon)\bar{y}b\,d\bar{y}. \tag{21}$$

Substituting the normal strain–curvature expression (6) and geometrical relation $\rho^{-1}(s) = \vartheta'(s)$ into Eq. (21) leads to

$$M_j(s) = \frac{1}{2}bD_{2,j}, \tag{22}$$

where

$$D_{2,j} = D_{2t,j} + D_{2c,j} + D_{2tc,j}, \tag{23}$$

$$D_{2t,j} = \sum_{i=1}^{j-1} E_{t,i}(h_{b,i}^2 - h_{t,i}^2)\varepsilon_{0t,i}^{1/k_{t,i}} - \sum_{i=1}^{j-1} \frac{2E_{t,i}k_{t,i}}{(1+k_{t,i})(1+2k_{t,i})\vartheta'(s)} \times \left(m_{tt,i}C_{tt,i}^{1+1/k_{t,i}} - m_{tb,i}C_{tb,i}^{1+1/k_{t,i}}\right), \tag{24}$$

$$D_{2c,j} = -\sum_{i=j+1}^{n} E_{c,i}(h_{b,i}^2 - h_{t,i}^2)\varepsilon_{0c,i}^{1/k_{c,i}} + \sum_{i=j+1}^{n} \frac{2E_{c,i}k_{c,i}}{(1+k_{c,i})(1+2k_{c,i})\vartheta'(s)} \times \left(-m_{ct,i}C_{ct,i}^{1+1/k_{c,i}} + m_{cb,i}C_{cb,i}^{1+1/k_{c,i}}\right), \tag{25}$$

$$D_{2tc,j} = E_{t,j}(a(s)^2 - h_{t,j}^2)\varepsilon_{0t,j}^{1/k_{t,j}} - E_{c,j}(h_{b,j}^2 - a(s)^2)\varepsilon_{0c,j}^{1/k_{c,j}} - \frac{2E_{t,j}k_{t,j}}{(1+k_{t,j})(1+2k_{t,j})\vartheta'(s)} \times \left[m_{tt,j}C_{tt,j}^{1+1/k_{t,j}} - \varepsilon_{0t,j}^{1+1/k_{t,j}}\left(\frac{k_{t,j}\varepsilon_{0t,j}}{\vartheta'(s)} + (1+2k_{t,j})a(s)\right)\right] + \frac{2E_{c,j}k_{c,j}}{(1+k_{c,j})(1+2k_{c,j})\vartheta'(s)} \times \left[m_{cb,j}C_{cb,j}^{1+1/k_{c,j}} + \varepsilon_{0c,j}^{1+1/k_{c,j}}\left(\frac{k_{c,j}\varepsilon_{0c,j}}{\vartheta'(s)} - (1+2k_{c,j})a(s)\right)\right], \tag{26}$$

$$m_{tt,i} = h_{t,i} + h_{t,i}k_{t,i} + k_{t,i}a(s) + \frac{k_{t,i}\varepsilon_{0t,i}}{\vartheta'(s)}, \tag{27}$$

$$m_{tb,i} = h_{b,i} + h_{b,i}k_{t,i} + k_{t,i}a(s) + \frac{k_{t,i}\varepsilon_{0t,i}}{\vartheta'(s)}, \tag{28}$$

$$m_{ct,i} = h_{t,i} + h_{t,i}k_{c,i} + k_{c,i}a(s) - \frac{k_{c,i}\varepsilon_{0c,i}}{\vartheta'(s)}, \tag{29}$$

$$m_{cb,i} = h_{b,i} + h_{b,i}k_{c,i} + k_{c,i}a(s) - \frac{k_{c,i}\varepsilon_{0c,i}}{\vartheta'(s)}. \tag{30}$$

3.3. *Derivative of the neutral axis position with respect to $s - a'(s)$*

Static equilibrium of an infinitesimal element of the deflected beam together with geometrical relations

$$x'(s) = \cos\vartheta(s) \quad \text{and} \quad y'(s) = \sin\vartheta(s), \tag{31}$$

see Fig. 5, results in

$$M'_j(s) + F_x(s)\sin\vartheta(s) + F_y(s)\cos\vartheta(s) = 0. \tag{32}$$

It can be observed, that in $M'_j(s)$ the derivative of the neutral axis position $a'(s)$ (which is in general unknown) appears. The influence of the inner axial force on the deformation of slender beams can be neglected as shown in Ref. [6]. By considering that the deformation of the beam is caused only by the inner bending moment it follows that the resultant in terms of force of normal stresses in any cross-section equals zero, i.e. $N_j(s) = 0$. Furthermore, from the derivative of the expression (7) with respect to s, i.e. $N'_j(s) = 0$, it can be found

$$a'_j(s) = \vartheta''(s)G_j, \tag{33}$$

where

$$G_j = -\frac{B_{1,j} + \vartheta'(s)B_{2,j}}{\vartheta'(s)^2 B_{3,j}}, \tag{34}$$

$$B_{2,j} = B_{2t,j} + B_{2c,j} + B_{2tc,j}, \tag{35}$$

$$B_{2t,j} = \sum_{i=1}^{j-1} E_{t,i}\left((h_{t,i} - a(s))C_{tt,i}^{1/k_{t,i}} - (h_{b,i} - a(s))C_{tb,i}^{1/k_{t,i}}\right), \tag{36}$$

$$B_{2c,j} = -\sum_{i=j+1}^{n} E_{c,i}\left((h_{t,i} - a(s))C_{ct,i}^{1/k_{c,i}} - (h_{b,i} - a(s))C_{cb,i}^{1/k_{c,i}}\right), \tag{37}$$

$$B_{2tc,j} = E_{t,j}(h_{t,j} - a(s))C_{tt,j}^{1/k_{t,j}} + E_{c,j}(h_{b,j} - a(s))C_{cb,j}^{1/k_{c,j}}, \tag{38}$$

$$B_{3,j} = B_{3t,j} + B_{3c,j} + B_{3tc,j}, \tag{39}$$

$$B_{3t,j} = -\sum_{i=1}^{j-1} E_{t,i}\left(C_{tt,i}^{1/k_{t,i}} - C_{tb,i}^{1/k_{t,i}}\right), \tag{40}$$

$$B_{3c,j} = \sum_{i=j+1}^{n} E_{c,i}\left(C_{ct,i}^{1/k_{c,i}} - C_{cb,i}^{1/k_{c,i}}\right), \tag{41}$$

$$B_{3tc,j} = E_{t,j}\left(\varepsilon_{0t,j}^{1/k_{t,j}} - C_{tt,j}^{1/k_{t,j}}\right) + E_{c,j}\left(\varepsilon_{0c,j}^{1/k_{c,j}} - C_{cb,j}^{1/k_{c,j}}\right). \tag{42}$$

3.4. *Derivative of the inner bending moment with respect to s — M′(s)*

$$M'_j(s) = \vartheta''(s)bD_{1,j}, \tag{43}$$

$$D_{1,j} = D_{1t,j} + D_{1c,j} + D_{1tc,j}, \tag{44}$$

$$\begin{aligned} D_{1t,j} = -\sum_{i=1}^{j-1} \frac{E_{t,i}}{(1+2k_{t,i})\vartheta'(s)^2}\Bigg[& \frac{k_{t,i}}{1+k_{t,i}} \\ & \times \left(-m_{tt,i}C_{tt,i}^{1+1/k_{t,i}} + m_{tb,i}C_{tb,i}^{1+1/k_{t,i}}\right) \\ & + \vartheta'(s)\left(-m_{gt,j,i}C_{tt,i}^{1/k_{t,i}}m_{tt,i} + m_{gb,j,i}C_{tb,i}^{1/k_{t,i}}m_{tb,i}\right) \\ & - \frac{k_{t,i}^2}{(1+k_{t,i})\vartheta'(s)}(\varepsilon_{0t,i} - G_j\vartheta'(s)^2)\left(C_{tt,i}^{1+1/k_{t,i}} - C_{tb,i}^{1+1/k_{t,i}}\right)\Bigg], \end{aligned} \tag{45}$$

$$\begin{aligned} D_{1t,j} = \sum_{i=j+1}^{n} \frac{E_{c,i}}{(1+2k_{c,i})\vartheta'(s)^2}\Bigg[& \frac{k_{c,i}}{1+k_{c,i}}\left(m_{ct,i}C_{ct,i}^{1+1/k_{c,i}} - m_{cb,i}C_{cb,i}^{1+1/k_{c,i}}\right) \\ & + \vartheta'(s)\left(-m_{gt,j,i}C_{ct,i}^{1/k_{c,i}}m_{ct,i} + m_{gb,j,i}C_{cb,i}^{1/k_{c,i}}m_{cb,i}\right) \\ & - \frac{k_{c,i}^2}{(1+k_{c,i})\vartheta'(s)}(\varepsilon_{0c,i} + G_j\vartheta'(s)^2)\left(C_{ct,i}^{1+1/k_{c,i}} - C_{cb,i}^{1+1/k_{c,i}}\right)\Bigg], \end{aligned} \tag{46}$$

$$m_{gt,j,i} = h_{t,i} - a(s) - G_j\vartheta'(s), \tag{47}$$

$$m_{gb,j,i} = h_{b,i} - a(s) - G_j\vartheta'(s), \tag{48}$$

$$\begin{aligned} D_{1tc,j} = {} & a(s)G_j\left(E_{t,j}\varepsilon_{0t,j}^{1/k_{t,j}} + E_{c,j}\varepsilon_{0c,j}^{1/k_{c,j}}\right) \\ & - \frac{E_{t,j}}{(1+3k_{t,j}+2k_{t,j}^2)\vartheta'(s)^3} \\ & \times \left[k_{t,j}\varepsilon_{0t,j}^{1+1/k_{t,j}}H_{1t,j} + C_{tt,j}^{1/k_{t,j}}[H_{2t,j} + k_{t,j}\vartheta'(s)H_{3t,j}]\right] \\ & - \frac{E_{c,j}}{(1+3k_{c,j}+2k_{c,j}^2)\vartheta'(s)^3} \\ & \times \left[k_{c,j}\varepsilon_{0c,j}^{1+1/k_{c,j}}H_{1c,j} + C_{cb,j}^{1/k_{c,j}}[H_{2c,j} + k_{c,j}\vartheta'(s)H_{3c,j}]\right], \end{aligned} \tag{49}$$

$$H_{1t,j} = \vartheta'(s)(a(s) - G_j\vartheta'(s))(1+2k_{t,j}) + 2k_{t,j}\varepsilon_{0t,j}, \tag{50}$$

$$\begin{aligned} H_{2t,j} = {} & h_{t,j}\vartheta'(s)^2(a(s) - h_{t,j} + G_j\vartheta'(s)) - 2k_{t,j}^2(\varepsilon_{0t,j} \\ & + a(s)\vartheta'(s))(\varepsilon_{0t,j} - G_j\vartheta'(s)^2), \end{aligned} \tag{51}$$

$$\begin{aligned} H_{3t,j} = {} & \vartheta'(s)(a(s)^2 - h_{t,j}^2 + G_j\varepsilon_{0t,j}) - 2h_{t,j}(\varepsilon_{0t,j} - G_j\vartheta'(s)^2) \\ & + a(s)(\varepsilon_{0t,j} + G_j\vartheta'(s)^2), \end{aligned} \tag{52}$$

$$H_{1c,j} = \vartheta'(s)(-a(s) + G_j\vartheta'(s))(1+2k_{c,j}) + 2k_{c,j}\varepsilon_{0c,j}, \tag{53}$$

$$\begin{aligned} H_{2c,j} = {} & h_{b,j}\vartheta'(s)^2(a(s) - h_{b,j} + G_j\vartheta'(s)) - 2k_{c,j}^2(\varepsilon_{0c,j} \\ & - a(s)\vartheta'(s))(\varepsilon_{0c,j} + G_j\vartheta'(s)^2), \end{aligned} \tag{54}$$

$$\begin{aligned} H_{3c,j} = {} & \vartheta'(s)(a(s)^2 - h_{b,j}^2 - G_j\varepsilon_{0c,j}) + 2h_{b,j}(\varepsilon_{0c,j} + G_j\vartheta'(s)^2) \\ & + a(s)(-\varepsilon_{0c,j} + G_j\vartheta'(s)^2). \end{aligned} \tag{55}$$

Finally, substituting Eq. (43) into Eq. (32), jth governing differential equation of the problem can be deduced in the following form

$$\vartheta''(s) = -\frac{F_x(s)\sin\vartheta(s) + F_y(s)\cos\vartheta(s)}{bD_{1,j}}, \tag{56}$$

where j, $j \in \{1, 2, \ldots, n\}$, depends on the neutral axis position $a(s)$ as it is described above and $D_{1,j} = f(\vartheta'(s))$. According to Figs. 1 and 5, the inner forces $F_x(s)$ and $F_y(s)$ are given by expressions

$$F_x(s) = -F_{0x} - \int_s^L q_x(s)\,ds \tag{57}$$

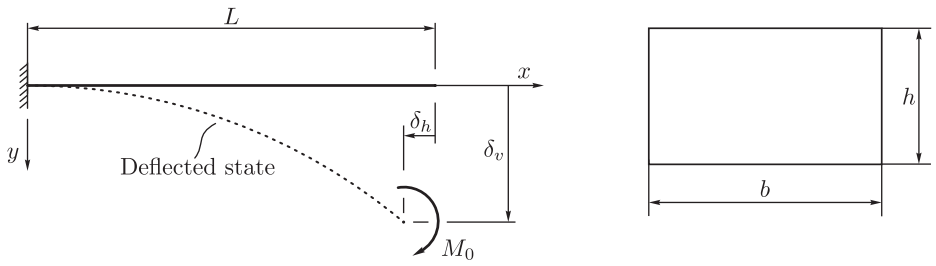

Fig. 6 – Cantilever beam subjected to an end moment M_0.

$$F_y(s) = F_{0y} + \int_s^L q_y(s)\, ds \tag{58}$$

respectively.

The governing second order nonlinear differential equation (56) is solved numerically using Runge–Kutta–Fehlberg (RKF) integration method together with accompanying initial conditions, i.e. $\vartheta(0) = 0$ and $\vartheta'(0) = \mu$, where μ is the unknown curvature of the deformed neutral axis at the clamped end. It should be noted, that $a(s)$ is solved numerically from Eq. (7) and $N_j(s) = 0$ whereas value of j is determined using Eq. (3) for each step of the RKF method. Since there is an unknown parameter in the numerical calculation, i.e. μ, the solution of $\vartheta(s)$ is obtained by employing the Newton's iterative method to satisfy the boundary condition at the free end within prescribed tolerance ε_p, i.e.

$$\begin{aligned} M_j(s = L) &= M_0, \\ \vartheta'(s = L) &= 0, \end{aligned} \tag{59}$$

if the cantilever beam is subjected or not to an end moment M_0, respectively. It should be mentioned that in the Newton's method the derivative is generated numerically using a fixed increment $\Delta\mu = 10^{-8}$. Furthermore, the Cartesian coordinate of the points along the neutral axis of the beam can be determined from the geometrical relations (31) and boundary conditions $x(s = 0) = 0$, $y(s = 0) = 0$.

4. Numerical examples

The equations and numerical procedure presented above were tested on several problems found in literature. The obtained deflection states are shown in the figures and tables below. The boundary condition at the free end is satisfied within a tolerance $\varepsilon_p = 10^{-9}$.

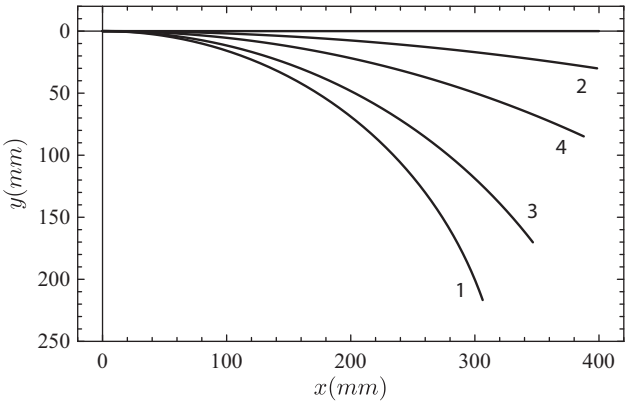

Fig. 7 – Deflected states of the cantilever beam subjected to an end moment (Baykara's problem).

4.1. *Example 1*

A nonlinear bimodulus cantilever beam of length $L = 400$ mm and uniform rectangular cross-section of thickness $h = 5$ mm and width $b = 20$ mm, which is subjected to an end moment $M_0 = 20 \times 10^3$ Nmm, Fig. 6, was investigated by Baykara et al. [5], where different material behaviour in tensile and compressive domain is considered.

For this case, where $n = 1$ and $h_1 = h$, in all numerical calculations, $E_{t,1}$ is taken to be 10^5 MPa. Since the Ludwick type of the stress–strain relationships is considered, the material constants $\varepsilon_{0t,1}$ and $\varepsilon_{0c,1}$ are set to be zero, i.e. $\varepsilon_{0t,1} = \varepsilon_{0c,1} = 0.0$. The vertical and horizontal deflections at the free end are for various material behaviour listed in Table 1, whereas the deflected states of the beam are shown in Fig. 7. A good agreement of the results can be observed.

If now length L, thickness h and width b of the beam are taken to be 1000 mm, 25 mm and 50 mm, respectively, and material constants as $E_{t,1} = E_{c,1} = 43.2735$ MPa, $k_{t,1} = k_{c,1} = 1.5$

Table 1 – Vertical and horizontal deflections at the free end.

#	$E_{c,1}$ (MPa)	$k_{c,1}$	$k_{t,1}$	δ_v (mm)	δ_v (mm) [5]	δ_h (mm)	δ_h (mm) [5]
1	50,000	0.8	1.0	216.706	216.70	93.713	93.71
2	25,000	2.0	1.0	29.995	29.99	1.503	1.503
3	75,000	1.0	0.8	170.202	170.20	53.258	53.25
4	25,000	1.0	2.0	84.840	84.83	12.259	12.25

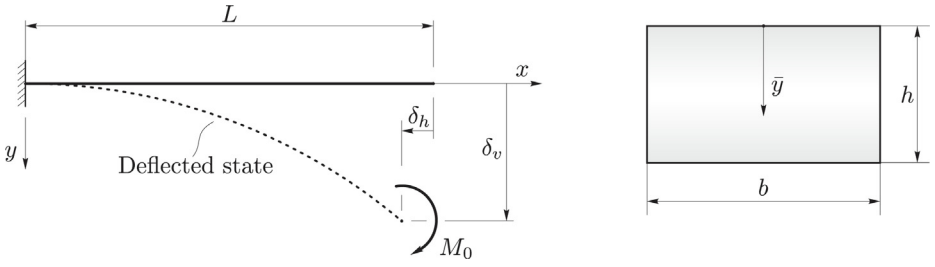

Fig. 8 – FGM cantilever beam subjected to an end moment M_0.

Table 2 – The radii of curvature.

#	M_0 ($\times 10^{-3}$ Nmm)	ρ (mm)	ρ (mm) [3]
1	1.0	4535.17	4535.17
2	10.0	435.212	435.212
3	200.0	13.7097	13.7097
4	600.0	3.07637	3.07637

Table 3 – Vertical deflections at the free end, $M_0 = 15 \times 10^3$ Nmm (example 2).

$k_{t,i} = k_{c,i}$	$\delta_{v,n=1}$ (mm)	$\delta_{v,n=4}$ (mm)	$\delta_{v,n=10}$ (mm)	$\delta_{v,n=40}$ (mm)
1/0.209	0.498	0.323	0.289	0.283
1/0.463	274.615	231.067	220.379	218.547

$k_{t,i} = k_{c,i}$	$\delta_{v,n=100}$ (mm)	$\delta_{v,n=400}$ (mm)	$\delta_{v,n=1000}$ (mm)	δ_v (mm) [15]
1/0.209	0.283	0.283	0.283	0.283
1/0.463	218.445	218.427	218.426	218.425

and $\varepsilon_{0t,1} = \varepsilon_{0c,1} = 0.07$, Brojan's problem is obtained, cf. [3]. The results of radii of curvature for various end moments are listed in Table 2. A perfect agreement of the results is observed.

4.2. *Example 2*

Kang and Li [15] presented results for large deflection of a nonlinear cantilever functionally graded material beam of length $L = 508$ mm and rectangular cross-section with $h = 6.35$ mm and $b = 25.4$ mm, subjected to an end moment $M_0 = 15 \times 10^3$ Nmm, see Fig. 8. The same relations in tensile and compressive domain are considered. The Young's modulus $E(\bar{y})$ of the FGM beam is assumed to vary over the beam thickness in a continuous way as follows

$$E(\bar{y}) = E_0\left(1 + \left|2\left(\frac{\bar{y}}{h} - \frac{1}{2}\right)\right|\right), \tag{60}$$

where $E_0 = 458.501$ MPa. In the present work this FGM beam is assumed to be composed of n laminae which are characterized by their constant thickness $\Delta = h/n$ and constant material properties. Accordingly, from the known expression for determining average value of a function for ith lamina it follows

$$E_{t,i} = E_{c,i} = \frac{1}{\Delta}\int_{(i-1)\Delta}^{i\Delta} E(\bar{y})\, d\bar{y}, \tag{61}$$

$i \in \{1, 2, \ldots, n\}$. The vertical and horizontal deflections at the free end upon the number of laminae n and material constants are presented in Tables 3 and 4, where the Ludwick type of the stress–strain relationships is considered ($\varepsilon_{0t,i} = \varepsilon_{0c,i} = 0.0$). Variation of the Young's modulus upon number of laminae n is depicted in Fig. 9. A good agreement of the results can be observed.

Table 4 – Horizontal deflections at the free end, $M_0 = 15 \times 10^3$ Nmm (example 2).

$k_{t,i} = k_{c,i}$	$\delta_{h,n=1}$ (mm)	$\delta_{h,n=4}$ (mm)	$\delta_{h,n=10}$ (mm)	$\delta_{h,n=40}$ (mm)
1/0.209	3.289×10^{-4}	1.385×10^{-4}	1.105×10^{-4}	1.063×10^{-4}
1/0.463	118.368	78.609	70.629	69.320

$k_{t,i} = k_{c,i}$	$\delta_{h,n=100}$ (mm)	$\delta_{h,n=400}$ (mm)	$\delta_{h,n=1000}$ (mm)
1/0.209	1.060×10^{-4}	1.060×10^{-4}	1.060×10^{-4}
1/0.463	69.248	69.235	69.234

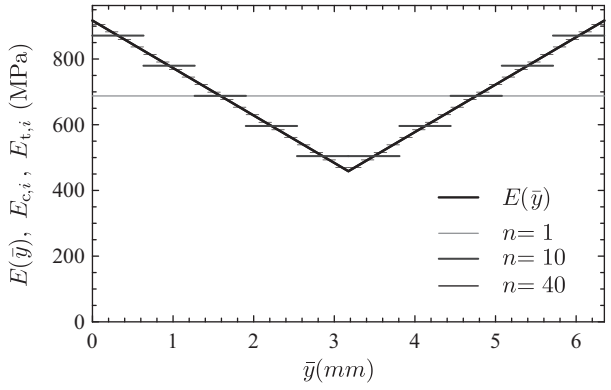

Fig. 9 – Young's modulus upon the number of laminae *n* (example 2).

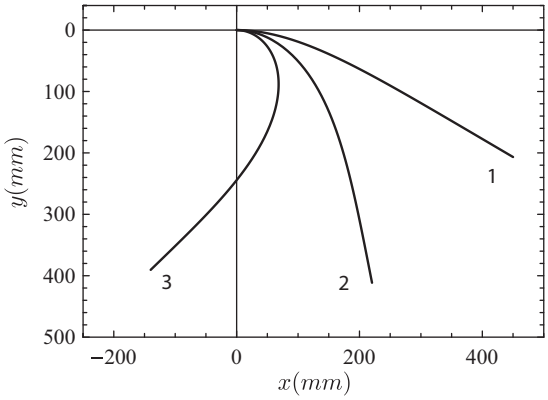

Fig. 11 – Deflected states of the cantilever beam subjected to a combined loading (*n* = 100).

4.3. *Example 3*

Fig. 10 shows a FGM cantilever beam of length $L = 500$ mm and rectangular cross-section with $h = 5$ mm and $b = 25$ mm, subjected to a combined load consisting of a linearly distributed vertical load $q_y(s) = s \times 0.25 \times 10^{-3}$ N/mm^2 and point load at the free end, i.e. F_{0x}.

The Young's modulus $E(\bar{y})$ of the FGM beam is assumed to vary over the beam thickness in a continuous way as follows

$$E(\bar{y}) = E_0\left(1 + \exp\left(-\gamma\left(\frac{\bar{y}}{h}\right)^{\beta}\right)\right), \tag{62}$$

where $E_0 = 458.501$ MPa, $\gamma = 13.4$ and $\beta = 1.8$. As in previous example, for ith lamina, $i \in \{1, 2, \ldots, n\}$, it follows $\Delta = h/n$ and $E_{t,i} = E_{c,i}$, where equation (61) is used. The remaining material constants are assumed to be $k_{t,i} = k_{c,i} = 2.3$ and $\varepsilon_{0t,i} = \varepsilon_{0c,i} = 6 \times 10^{-5}$. The vertical and horizontal deflections at the free end upon the number of laminae *n* and applied end load are listed in Tables 5 and 6, whereas the deflected states of the beam are shown in Fig. 11. Variation of the Young's modulus upon number of laminae *n* is depicted in Fig. 12.

4.4. *Example 4*

In particular, taking $L = 500$ mm, rectangular cross-section with $h = 20$ mm, $b = 10$ mm and a constantly distributed vertical load $q_y(s) = 75$ N/mm, cf. Fig. 13, a special case considered in Ref. [18] is obtained.

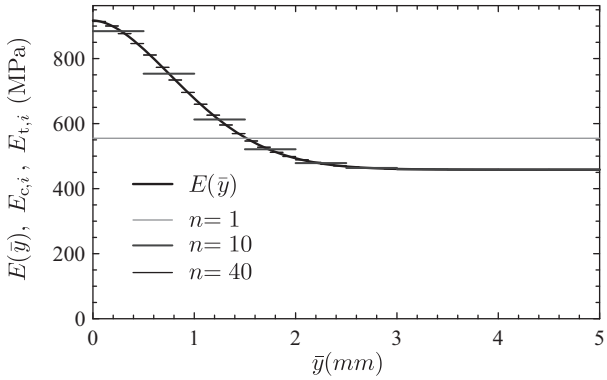

Fig. 12 – Young's modulus upon the number of laminae *n* (example 3).

The Young's modulus $E(\bar{y})$ is assumed to vary over the beam's thickness in a continuous way as follows

$$E(\bar{y}) = (E_t - E_b)\left(-\frac{\bar{y}}{h} + 1\right)^{\beta} + E_b, \tag{63}$$

where $E_t = 151$ MPa and $E_b = 70$ MPa and represent Young's modulus of the top and the bottom surfaces of the beam, respectively. Hooke's type of material and the same relations

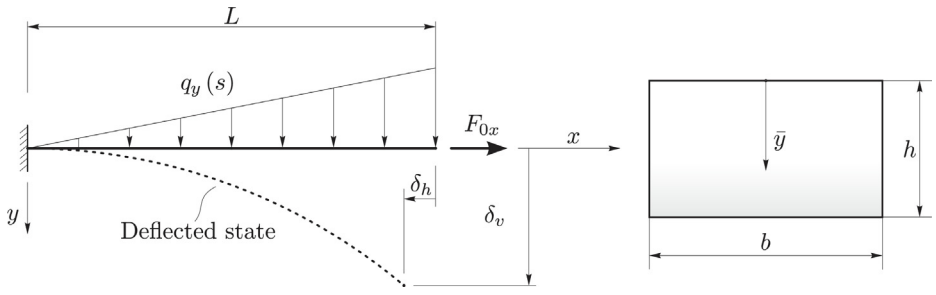

Fig. 10 – FGM cantilever beam subjected to a combined loading.

Table 5 – Vertical deflections at the free end, $q_y(s) = s \times 0.25 \times 10^{-3}$ N/mm^2 (example 3).

#	F_{0x} (N)	$\delta_{v,n=1}$ (mm)	$\delta_{v,n=10}$ (mm)	$\delta_{v,n=40}$ (mm)	$\delta_{v,n=100}$ (mm)
1	0.0	222.010	207.452	206.730	206.690
2	−20.0	422.160	412.039	411.463	411.431
3	−50.0	383.398	390.101	390.434	390.453

Table 6 – Horizontal deflections at the free end, $q_y(s) = s \times 0.25 \times 10^{-3}$ N/mm^2 (example 3).

#	F_{0x} (N)	$\delta_{h,n=1}$ (mm)	$\delta_{h,n=10}$ (mm)	$\delta_{h,n=40}$ (mm)	$\delta_{h,n=100}$ (mm)
1	0.0	58.143	50.340	49.970	49.950
2	−20.0	309.676	281.045	279.582	279.501
3	−50.0	655.221	640.705	639.954	639.913

Table 7 – Vertical and horizontal deflections at the free end, $n = 400$ (example 4).

#	β	δ_v (mm)	δ_v (mm) [18]	δ_h (mm)
1	0	341.043	341.628	160.770
2	0.3	361.960	361.759	187.369
3	1	382.002	381.061	216.889
4	3	393.309	392.313	235.719
5	$E(\bar{y}) = E_b$	415.231	416.287	278.004

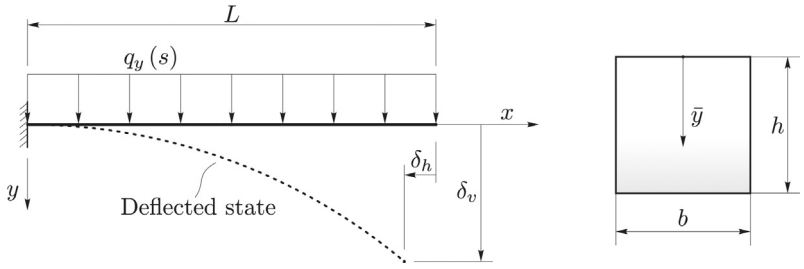

Fig. 13 – FGM cantilever beam subjected to a constantly distributed vertical load.

in tensile and compressive domain are considered ($E_{t,i} = E_{c,i}$, $k_{t,i} = k_{c,i} = 1$ and $\varepsilon_{0t,i} = \varepsilon_{0c,i} = 0$, $i \in \{1, 2, \ldots, n\}$). The vertical and horizontal deflections at the free end are listed in Table 7, whereas the variation of the Young's modulus is depicted in Fig. 14. Although Kocatürk et al. [18] have solved this problem using Timoshenko beam theory and finite element method, a good agreement of the results can be observed, since the beam is still relatively thin, cf. Table 7.

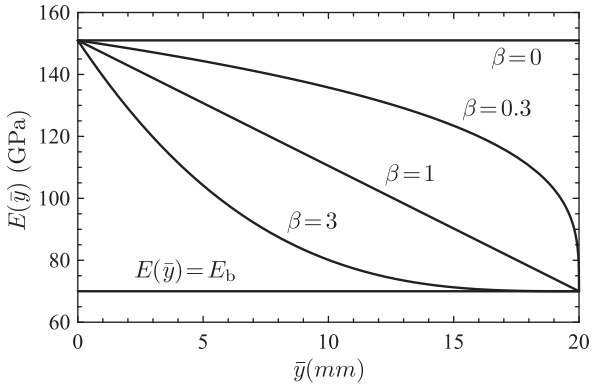

Fig. 14 – Variation of the Young's modulus (example 4).

5. Conclusion

The study discusses large deflections of slender, non-homogeneous cantilever beams subjected to a combined loading consisting of the distributed continuous loads and point loads at the free end. An exact inner axial force, inner bending moment, derivative of the neutral axis position and derivative of the inner bending moment with respect to the curvilinear coordinate as a function of curvature formulas are derived for uniform rectangular non-homogeneous beams composed of a finite number of laminae. Each lamina is made of nonlinearly elastic, modified Ludwick's type of material with different stress–strain relations in tension and compression domain. In the case when the material properties vary through the beam's thickness, the deflected states depending upon the number of laminae are presented. A good agreement with the results from the previously published studies has been established. When the thickness of laminae is sufficiently small and the variation of material properties in the laminae is (close to)

continuous, the beam can be considered as to be made of functionally graded material.

The presented governing differential equations can be used successfully for determining large deflections of beams made of modified Ludwick's, Ludwick's or Hooke's type of material, with arbitrary FGM distribution function. To investigate the beams with arbitrary boundary conditions, differential equations for both positive and negative curvature of the deformed neutral axis may be introduced in a similar manner as shown in this paper for the cantilever example.

Acknowledgement

Miha Brojan gratefully acknowledges The Fulbright Program financial support in the academic year 2012/2013.

REFERENCES

[1] G. Lewis, F. Monasa, Large deflections of cantilever beams of non-linear materials of the Ludwick type subjected to an end moment, International Journal of Non-Linear Mechanics 17 (1) (1982) 1–6.
[2] K. Lee, Large deflections of cantilever beams of non-linear elastic material under a combined loading, International Journal of Non-Linear Mechanics 37 (3) (2002) 439–443.
[3] M. Brojan, T. Videnic, F. Kosel, Large deflections of nonlinearly elastic non-prismatic cantilever beams made from materials obeying the generalized Ludwick constitutive law, Meccanica 44 (6) (2009) 733–739.
[4] M. Brojan, M. Sitar, F. Kosel, On static stability of nonlinearly elastic Euler's columns obeying the modified Ludwick's law, International Journal of Structural Stability and Dynamic 12 (6) (2012).
[5] C. Baykara, U. Güven, I. Bayer, Large deflections of a cantilever beam of nonlinear bimodulus material subjected to an end moment, Journal of Reinforced Plastics and Composites 24 (12) (2005) 1321–1326.
[6] M. Brojan, M. Cebron, F. Kosel, Large deflections of non-prismatic nonlinearly elastic cantilever beams subjected to non-uniform continuous load and a concentrated load at the free end, Acta Mechanica Sinica 28 (3) (2012) 863–869.
[7] S. Al-Sadder, N. Shatarat, A proposed technique for large deflection analysis of cantilever beams composed of two nonlinear elastic materials subjected to an inclined tip concentrated force, Advances in Structural Engineering 10 (3) (2007) 319–335.
[8] S. Suresh, Modeling and design of multi-layered and graded materials, Progress in Materials Science 42 (1–4) (1997) 243–251.
[9] B.V. Sankar, An elasticity solution for functionally graded beams, Composites Science and Technology 61 (5) (2001) 689–696.
[10] Z. Zhong, T. Yu, Analytical solution of a cantilever functionally graded beam, Composites Science and Technology 67 (3–4) (2007) 481–488.
[11] Z. Zhong, T. Yu, Two-dimensional analysis of functionally graded beams, AIAA Journal 44 (12) (2007) 3160–3164.
[12] G.J. Nie, Z. Zhong, S. Chen, Analytical solution for a functionally graded beam with arbitrary graded material properties, Composites Part B: Engineering 44 (1) (2013) 274–282.
[13] A. Chakraborty, S. Gopalakrishnan, J.N. Reddy, A new beam finite element for the analysis of functionally graded materials, International Journal of Mechanical Sciences 45 (3) (2003) 519–539.
[14] X.-F. Li, A unified approach for analyzing static and dynamic behaviors of functionally graded Timoshenko and Euler–Bernoulli beams, Journal of Sound and Vibration 318 (4–5) (2008) 1210–1229.
[15] Y.-A. Kang, X.-F. Li, Large deflections of a non-linear cantilever functionally graded beam, Journal of Reinforced Plastics and Composites 29 (12) (2010) 1761–1774.
[16] Y.-A. Kang, X.-F. Li, Bending of functionally graded cantilever beam with power-law non-linearity subjected to an end force, International Journal of Non-Linear Mechanics 44 (6) (2009) 696–703.
[17] J.H. Jung, T.J. Kang, Large deflection analysis of fibers with nonlinear elastic properties, Textile Research Journal 75 (10) (2005) 715–723.
[18] T. Kocatürk, M. Şimşek, S.D. Akbaş, Large displacement static analysis of a cantilever Timoshenko beam composed of functionally graded material, Science and Engineering of Composite Materials 18 (1–2) (2011) 21–34.
[19] A. Soleimani, Large deflection of various functionally graded beam using shooting method, Applied Mechanics and Materials 110–116 (2012) 4705–4711.
[20] A. Soleimani, M. Saddatfar, Numerical study of large defection of functionally graded beam with geometry nonlinearity, Advanced Materials Research 403–408 (2012) 4226–4230.